Bearing diagnostics and speed estimation via smartphone standalone data

Alexandre Mauricio, Toby Verwimp, Konstantinos Gryllias

Bearing diagnostics and speed estimation via smartphone standalone data

Alexandre MAURICIO[1,2], Toby VERWIMP[1,2], Konstantinos GRYLLIAS[1,2]

[1]KU Leuven, Department of Mechanical Engineering
LMSD Division Mecha(tro)nic System Dynamics
Celestijnenlaan 300, B-3001, Heverlee, Belgium
[2]Flanders Make @ KU Leuven, Belgium
alex.ricardomauricio@kuleuven.be

Abstract

Condition monitoring of rolling element bearings is a point of interest for early damage detection and prediction to avoid unexpected rotating machinery breakdown. Rolling element bearing related signals are often acquired with accelerometers, as vibration signals usually carry sensitive early information related to the bearing damages. However the accelerometers need to be physically mounted in contact near the bearing to be monitored. Acoustics signals from microphones provide an alternative solution as they acquire signals from multiple sources and bearings, without needing to be in contact with the bearing housing. Accurate speed estimation is also a necessity for detection of the bearing damages, as the bearing related frequencies are dependent of the shaft speed. Encoders are then needed to be added during design phase and mounted to the drivetrain, or a zebra tape and optical tachometer are glued and mounted on one shaft of the drivetrain to properly extract the speed signal. Instead of using expensive data acquisition systems to monitor the health status of rolling element bearings, the use of smartphone standalone data is proposed. The shaft speed extraction is based on video images acquired by the smartphone camera. This methodology exploits the deformation of the video image due to the rolling shutter effect of the smartphone camera. The bearing damage detection is based on the audio of the smartphone video. The audio is captured in stereo by a dual plug-in microphone. The speed estimation via video and signal processing methodologies proposed for bearing diagnostics are applied on real data captured from an experimental drivetrain with different cases of damaged bearings running at varying shaft speeds in the range of 5 to 40 revolutions per second.

1 Introduction

In order to monitor the health status of an industrial machine it is required to know the characteristic frequencies of the machine parts. Based on those characteristic frequencies it is possible to detect if a machine part is defected and to identify the machine component.

Vibration analysis is often performed to detect the modulations of the vibration signal induced by the existence of defects or misalignments of certain machine components. The faulty component and the severity of the fault can be determined by examining the characteristic frequencies of the different machine parts. When the damage related signatures are hidden under the noise level of the signal, it is common practice to filter around the carrier band excited by the damage, and apply the Hilbert transform to obtain the envelope spectrum with the modulations of interest for bearing diagnostics [1]. Frequency-frequency methods such as the Spectral Correlation have also been proposed as robust methods that exhibit the masked modulations in a bi-frequency map [2]. However these methods assume a steady rotating speed. Abboud *et al.* [3, 4] proposed an extension of the method, where the angular resampling procedure with the known varying speed profile Is applied in order to obtain the Order-Frequency Spectral Correlation or Coherence map. In this case, the cyclic modulations of the bearing faults would be represented as a function of the shaft angle to provide robust bearing diagnostics under varying speed conditions.

Vibration signals can be measured by using accelerometers. One downside of using vibration measurements is the placement of the accelerometers. They have to be attached to the machine structure and can thereby not be placed directly onto the rotating machine parts.

Acoustic non-contact sensors such as microphones recently drew attention as an alternative to accelerometers, as they do not need to be physically mounted by bolts, glue or magnets. Additionally microphone acoustic signals may also acquire information of several sources. These sources could be other potential bearing signatures, along with other additional undesirable noise sources. For this reason, further dedicated methods to further enhance the bearing impulses in microphone signals are a necessity [5]. One proposal to improve the signal to noise ratio of bearing damages hidden in the signals is to increase the number of microphones in an array with known spatial coordinates and apply sum-and-delay beamforming [6] or to use the kurtosis as an indicator for damage localization [7]. These methods have also recently been extended for varying speed conditions [8, 9].

Under varying speed conditions, the speed measurements need to be acquired and synchronized with the sensor signals from the microphones. In normal circumstances, a dedicated data acquisition system connected to high end microphones, accelerometers, tachometer or encoders is used to acquire the speed reference and the signals for diagnostics. On the other hand, with the the increase in computational power, smartphones contain multiple sensors, such as gyroscopes, accelerometers and microphones, as well as high resolution cameras.

Data acquired through widely available smartphones can provide a cheaper solution in relation to expensive classical data acquisition systems. Recently, the video data of a rotating shaft with a zebra tape glued onto it has been successfully used to estimate accurately the speed conditions of the rotating machinery [10, 11, 12].

This paper proposes using the smartphone sensors and its synchronized standalone data for bearing diagnostics, as opposed to the classical data acquisition systems and high end sensors. The speed reference is estimated with image processing methods proposed by Toby *et. al.*[11, 12], and the audio data from the microphones processed using the estimated speed and the integration of the Order-Frequency Cyclic Modulation Spectrum (OFCMS) proposed by Abboud *et al.* [3, 4]. Bearings diagnostics using the smartphone standalone data is validated on an experimental setup under varying speed, with three different bearing damaged cases (inner race, outer race and healthy).

2 Speed estimation with image processing

The speed extraction is usually performed with an encoder or a tachometer mounted to a shaft, where radial increments are mounted, like a zebra tape. Knowing the specific angle of each tracked increment and the time stamp, the derivative can be extracted, resulting in the speed signal.

Smartphone video data is usually acquired via a rolling shutter instead of a global shutter. The rolling shutter acquires one row at the time on each photo, and it is used to decrease the computing power needed to acquire high resolution pictures. In contrast, this also results in deformation of the picture due to the rolling shutter effect.

On the SURVISHNO challenge of 2019 [10] the rolling shutter was proposed to be used to track and estimate the rotational speed of a hydraulic fan filmed from an axial perspective. More recently, Toby *et al.* [11, 12] proposed to use a zebra tape glued to the shaft and acquire the video of the zebra tape from a radial position. Taking advantage of the rolling shutter effect, the deformation of the zebra stripes can be tracked, and the speed ω can be estimated as a function of the angle α, as described in Fig. 1.

Secondly, a video of a calibration pattern held in front of the shaft is required to calibrate the distance between the camera and the shaft. Finally, a video of the rotating shaft is required to extract the deformation angle of the stripes on the zebra pattern and calculate the shaft speed.

The angle β between the shaft axis and the rolling shutter direction also influences the speed estimation and needs to be measured. This can be done by image processing, by acquiring the shaft pixels in one photo and measuring the angle.

The speed estimation is also function of the rolling shutter period τ, which can be calculated by acquiring the video of a blinking LED light at a known frequency.

Lastly, the distance from the zebra pattern to the camera Z, the number of vertical pixels per unit length k_y and the focal length f_y are also needed to be measured. A video of a calibration pattern held in front of the shaft is required to calibrate the distance between the camera and the shaft. Once these parameters are known and

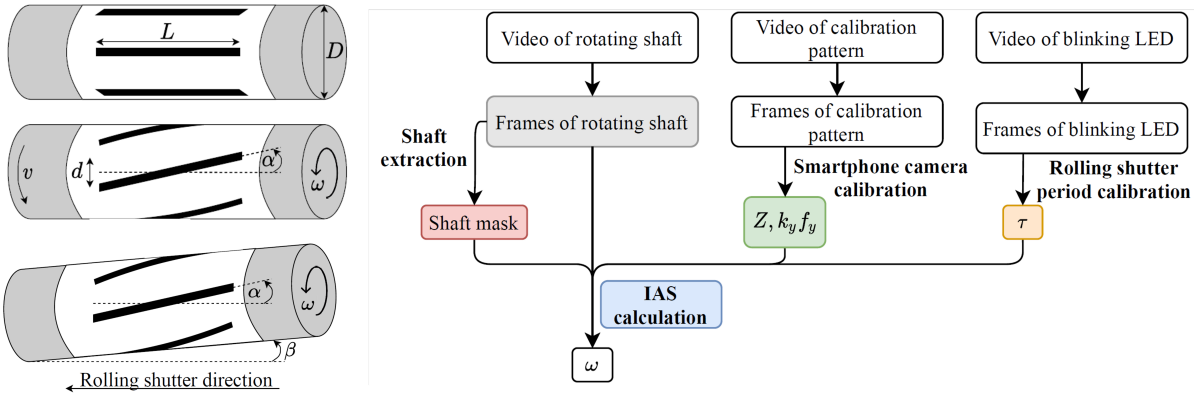

Figure 1: Flowchart of the methodology to extract the speed from a radial viewpoint

calibrated, the rotational speed ω of the shaft can be calculated as:

$$\omega = \frac{1}{\pi D \tau} \frac{Z}{k_y f_y} (tan(\alpha) cos(\beta) - sin(\beta)) \tag{1}$$

where α is the angle of the stripes from the zebra pattern, β takes into account the misalignment of the shaft. In Figure 1 an overview of the methodology to extract the shaft speed is given.

3 Bearing diagnostics with acoustic signals

Rotating mechanical components are likely to generate cyclic transient signatures which are periodic in nature if the signals were acquired under constant rotational speed. The cyclic transient signatures carry information on the health of machinery components. Signal processing and feature extraction are widely used in order to extract the repetitive transients for diagnosis and prognosis. The vibration signals are usually classified as first order or second order cyclostationary.

In rotating machinery, first-order cyclostationary vibrations signals are periodic waveforms related to components phase-locked with the rotor speed (*e.g.* shaft misalignment, spalling on meshing gears, etc.). On the other hand, second-order cyclostationary signals have periodic second order statistical moments [2]. Bearing vibration signals are often described as C_2, due to having a hidden periodicity related to the shaft speed.

The Spectral Correlation (SCor) is a tool where the first-order and second-order cyclostationary signals are well described in the frequency-frequency domain. The method is represented as a distribution function of two frequency variables: the *cyclic frequency* α linked to the modulation and the *spectral frequency* f linked to the carrier signal. The tool can be described also as the correlation distribution of the carrier and modulation frequencies of the signatures present in the signals, defined in Eq. 2:

$$SCor(\alpha, f) = \lim_{W \to \infty} \frac{1}{W} E\{F_W[x(t)] F_W[x(t+\tau)]^*\} \tag{2}$$

where t stands for the time and W stands for the cycle period, τ corresponds to the time-lag variable, and $F_W[x(t)]$ stands for the Fourier transform of the signal $x(t)$ over a finite time duration of W. Processing the SCor results in a bi-variable map, which reveals the hidden modulations, making it a robust tool for detecting the cyclostationarity in vibration signals [2].

Signals with a hidden periodicity related to the shaft angle can be defined as cyclostationary in time under constant speed operating conditions. However, the periodicity of the impulses is dependent on the shaft speed, while the carriers are often time-invariant. Thus, they are defined as non-stationary. This signal nature is known to be the definition of the signal of rolling element bearings under varying operating conditions. Although the signals are neither time nor angle-cyclostationary, a hidden periodicity is still present in the signal. These signals are classified as Cyclo-Non-Stationary (CNS) signals, and some order tracking techniques can be applied to the bi-variable map.

CNS signals with time-invariant phenomena result in a distortion along the spectral variable order axis f. In alternative, the so called "angle-time cyclostationary" (AT-CS) [3, 4] processes can be applied in order to extract a bi-variable function of angle in the cyclic variable axis α and function of time in the spectral variable axis f. This prevents the distribution of the time-invariant carrier coefficients to smear along the spectral axis, as well as preventing the distribution of the angle-invariant modulation coefficients to smear along the cyclic axis. The angle-time cyclostationary process can be defined as the correlation between two time instants locked in angle position θ and spaced by the time-lag τ. Therefore, the correlation function between $t(\theta)$ and $t(\theta)-\tau$ results in the SCor function in the Order-Frequency domain $OFSCor$ as defined in Eq. 3:

$$OFSCor(\alpha(\theta), f(t)) = \lim_{W\to\infty} \frac{1}{W} E\{F_W[x(t(\theta))]F_W[x(t(\theta)+\tau)]^*\} \tag{3}$$

where the cyclic variable α is a function of the angle θ, while the spectral variable f is a function of time t.

In order to minimize uneven distributions over the spectral frequency axis, a whitening operation can be applied to the OFSCor. Normalizing the map by the Power Spectrum at cyclic frequency $\alpha = 0$ to obtain the Order Frequency Spectral Coherence (OFSCoh) describes the spectral correlations in normalized values, and has a magnitude between 0 and 1. The OFSCoh is defined in Eq. 4:

$$OFSCoh(\alpha, f) = \frac{OFSCor(\alpha, f)}{\sqrt{OFSCor(0, f)OFSCcor(0, f+\alpha)}} \tag{4}$$

Both the OFSCor and the OFSCoh bi-variable maps can be integrated along the spectral frequency axis in order to obtain a regular spectrum, resulting in a one dimensional spectrum over the cyclic frequency α.

The integration band over spectral frequencies can be defined as the full available band, i.e. from zero up to the Nyquist frequency, resulting in a spectrum that exhibits all modulations present in the signal. The resulting spectrum is referred to as the Enhanced Envelope Spectrum (EES) and it is obtained from the order-frequency OFSCoh according to Eq. 5:

$$EES(\alpha) = \frac{1}{Fs}\int_0^{Fs/2} |OFSCoh(\alpha, f)| df \tag{5}$$

In fact, the same procedure can also be performed on the original frequency-frequency domain SCor, however that method is only valid when assuming steady speed conditions. As this paper focuses on signals under varying speed conditions, angular-time transformation procedures to work on order-frequency domain are needed.

In this paper, the Order-Frequency Spectral Coherence and its Enhanced Envelope Spectrum by integration of its full spectral band are proposed to obtain the cyclo-non-stationary signatures related to the bearing damages. The bi-variable functions in the order-frequency domain are extracted using the Order-Frequency Cyclic Modulation Spectrum (OFCMS) estimation proposed by Abboud et al. [4]

4 Experimental setup and results

In this section a run through of the experimental campaign is given. First the experimental setup that was required to do the measurements is shown, followed by the results for the outer race damage, inner race damage and healthy conditions.

The experimental test setup corresponds to a speed controlled motor coupled with a shaft supported by 2 bearings, of which one is the tested bearing containing different damage conditions. The front view and side are shown in Fig. 2. All key elements that are required to perform the experiments are highlighted with a number ranging from 1 to 17.

The WEG 1.5 kW induction speed controlled motor (1) drives the shaft (4) via a CFW500 driver. The bearings supporting the shaft are both SKF 2206 EKTN9 self aligning bearings. Different damages of different severities were tested and mounted on position (3). The damages correspond to a Small Outer Race (SOR) damage, a Mild Inner Race (MIR) damage and a Large Outer Race (LOR) damage that can be seen in Fig. 3.

A laser tachometer (18) is used to acquire the reference speed to be used as a benchmark, and three high end microphones from PCB Piezotronics (7, 8, 9) are used as the reference acoustic signals. Two uniaxial

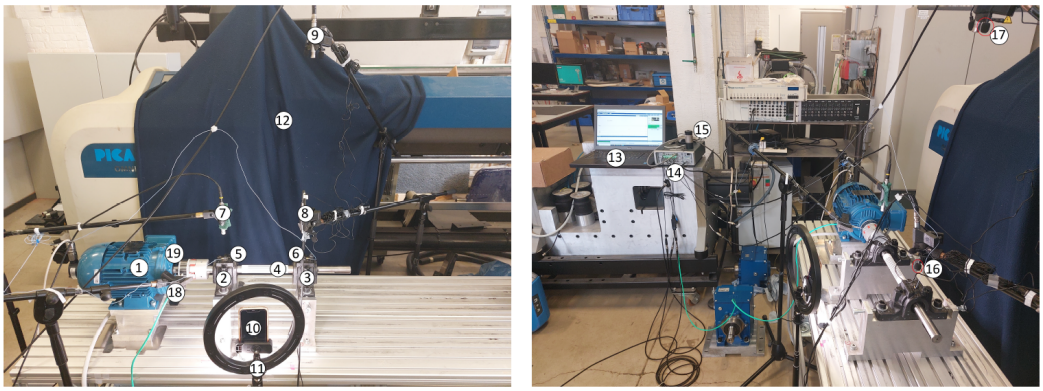

Figure 2: (A) Front view and (B) side view of the experiment setup

accelerometer signals were also captured during testing. The signals were acquired using a SCADAS system (14) at 51.2 kHz sampling frequency.

A simple printed zebra (4) is glued to the drive shaft for the speed estimation using the video acquired by the smartphone (10) mounted on a DC LED light stand (11). Two Lavalier microphones (16, 17) are used to acquire the acoustic signals by the smartphone.

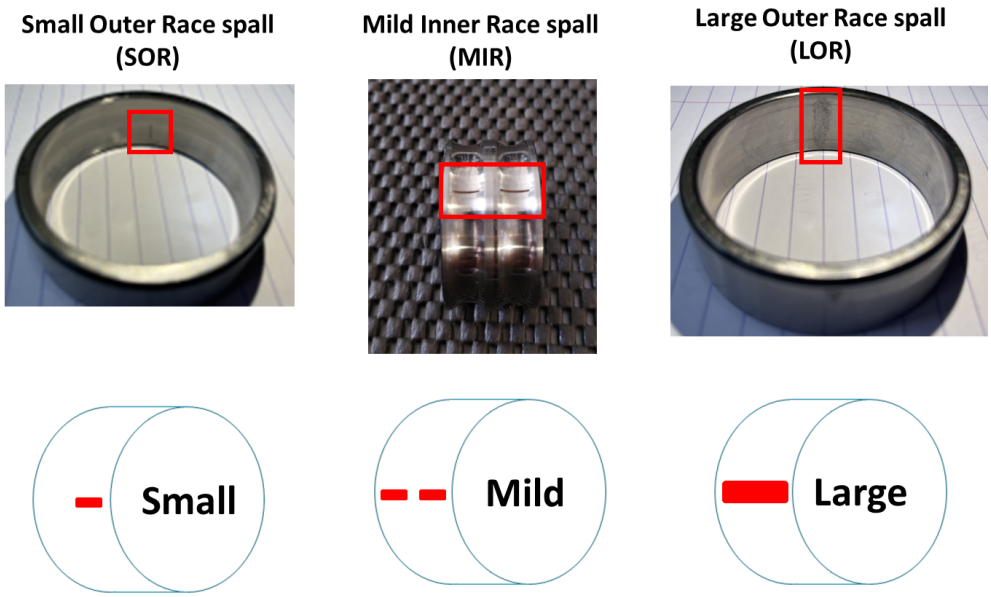

Figure 3: (A) Front view and (B) side view of the experiment setup

Each test run started by turning on the motor power and running the shaft at steady 5 rps speed. Once the shaft was at steady speed, the acquisition on the SCADAS and the smartphone video started. Next, a hand clap is performed in the beginning of the acquisition for synchronization purposes between all microphone signals. After the clap the shaft runs at a steady speed of 5 rps for 5 seconds straight. Thereafter the shaft speed was increased to 10 rps and kept running for another 5 seconds. The same procedure is repeated when increasing the speed subsequently to 20, 30 and 40 rps. After the completion of the shaft running at 40 rps for 5 seconds straight, the shaft speed is gradually decreased to the stationary speed of 5 rps.

The speed profile corresponding to the LOR case following these conditions can be seen in Fig. 4. The speed profile shown in red corresponds to the reference benchmark speed extracted from the laser tachometer, and the speed profile in black corresponds to the speed profile estimated with the image processing method.

Here it can be seen that the estimated speed is rather accurate, as it only shows small deviations and errors corresponding to the reference speed.

The high end microphone and smartphone acoustic data for the LOR damaged bearing is shown in Fig. 4. It is important to note that the acoustic signal corresponds to units measured in Pascal, as the microphones have been calibrated and no pre-processing has been performed. On the other hand the smartphone microphones have in-built pre-processing steps that normalize and filter the signals, which corresponds in different signals as exhibited in Fig. 4.

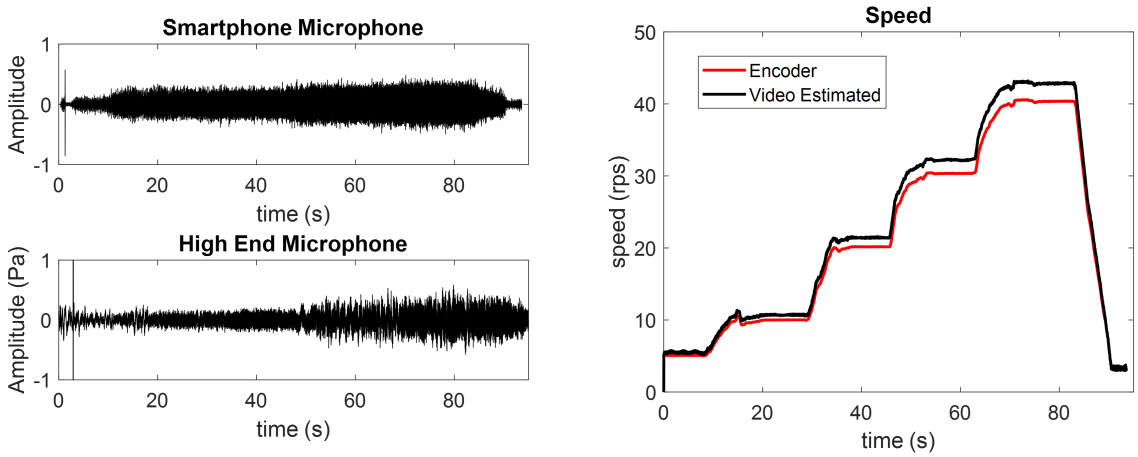

Figure 4: Raw acoustic signal for a LOR damaged bearing from (top) Smartphone microphone and (bottom) High End microphone.

One such difference occurs in frequencies above 14.5 kHz, where the spectral content is removed from the audio data. This is due to the audio compression algorithms used to reduce the file size of the smartphone video recording. The loss of the high frequency spectrum may complicate the detection and identification of bearing damages.

Next is the the analysis of the diagnostics results. Extraction of the Order-Frequency bi-variable map (OFCMS) of the smartphone microphone signals using the speed estimated is shown in Fig. 5.

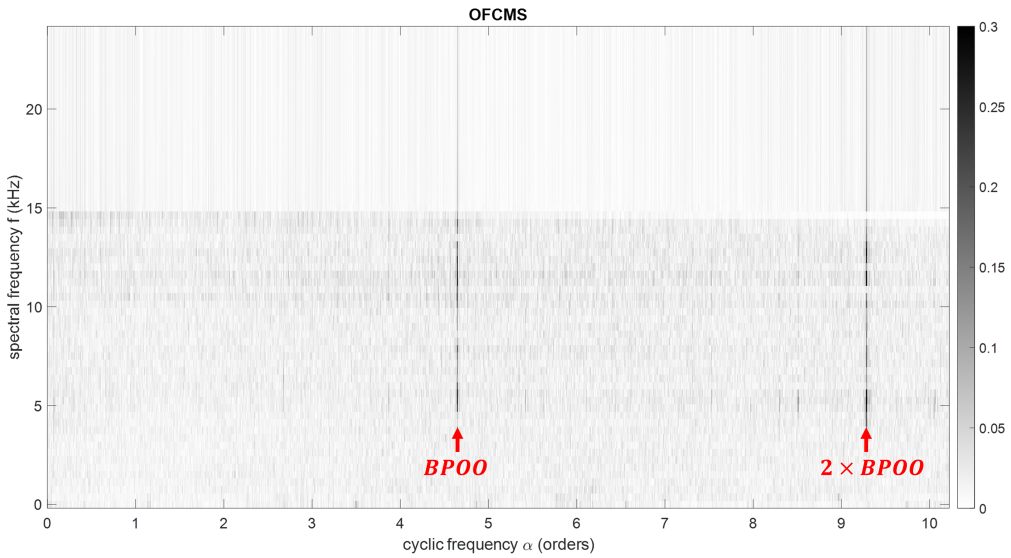

Figure 5: Order-Frequency Spectral Coherence (OFCMS) of the smartphone acoustic signal for the large outer race damage case.

The OFCMS exhibits the order harmonics corresponding to the outer race, the Ball Pass Order of Outer race

(BPOO). The amplitude of these harmonics are also clearly above the background noise level. The OFCMS also shows that components above 14.5 kHz are not present due to the compression processing of the signals.

Integration of full spectral band of the OFCMS results in the EES where the 3 BPOO harmonics are detected above the background noise level, as shown in Fig. 6. This results in a clear diagnostics of damage on the outer race of the bearing.

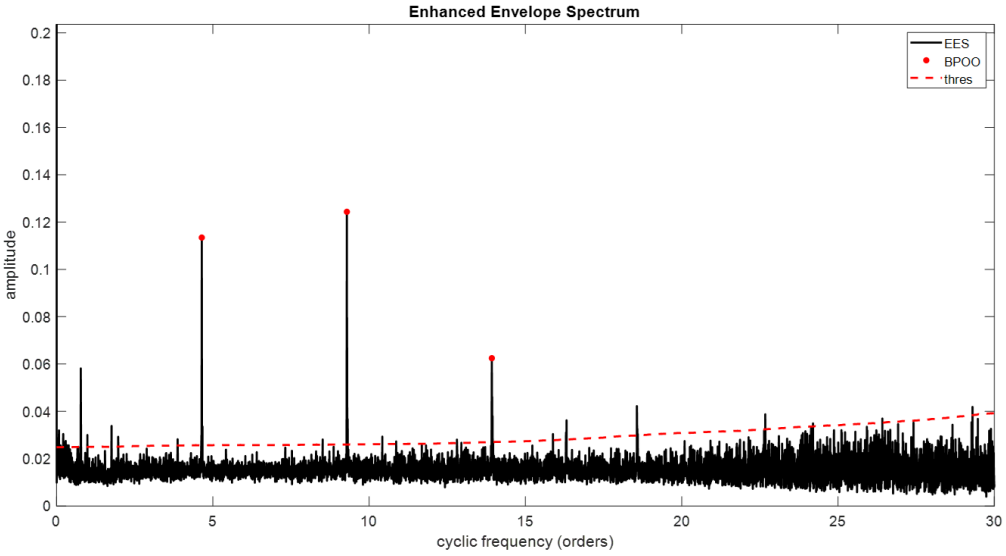

Figure 6: Enhanced Envelope Spectrum from the OFCMS of the smartphone acoustic signal for the large outer race damage case.

Following the case of the inner race bearing, the smartphone and high end microphone acoustic signals along with the reference speed and the estimated speed are shown in Fig. 7.

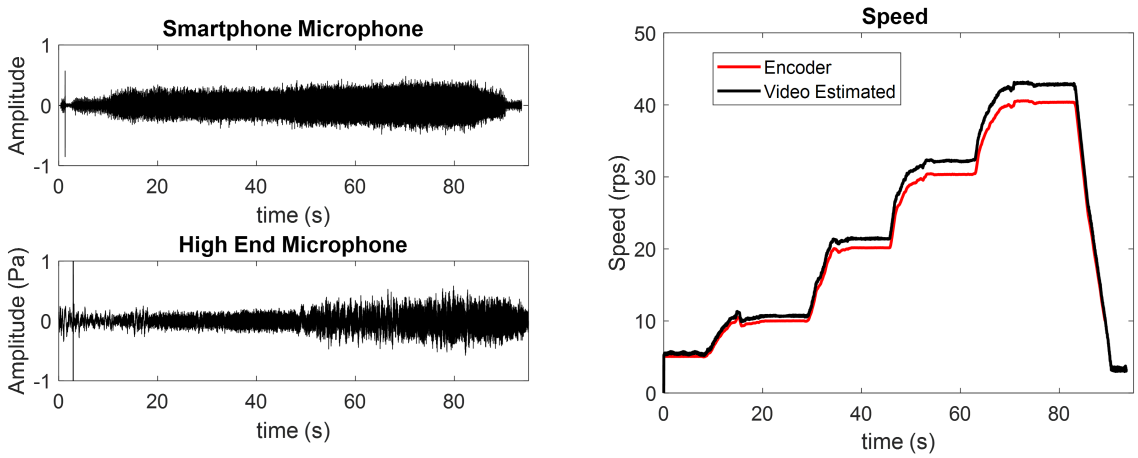

Figure 7: (left) Acoustic signals from high end and smartphone microphones and (right) speed from image processing estimation and reference speed from encoder.

Here it can be seen that the proposed method for speed estimation overestimated the speed, which may be due to error during the acquisition or the video calibration. This speed estimation error results in a higher cyclo-non-stationarity of the impulses of the localized inner race damage, which occur more randomly in the angle domain, due to the angle-resampling step of the OFCMS being performed with an inaccurate speed measurement. The resulting smearing of the amplitudes of Ball Pass Order of the Inner race (BPOI) and its sidebands seen in Fig. 8 are due to this effect.

Accurate speed estimation is needed for bearing diagnostics under varying speed conditions which use

angular resampling methods. However, the speed estimation error is small enough that the BPOI harmonics and its sidebands are still detected above the noise level of the OFCMS and its EES, shown in Fig. 9.

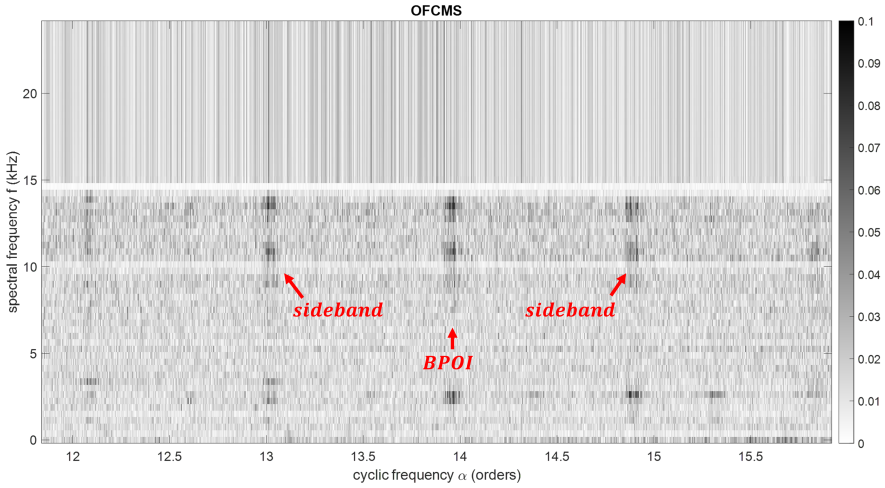

Figure 8: Order-Frequency Spectral Coherence (OFCMS) of the smartphone acoustic signal for the mild inner race damage case.

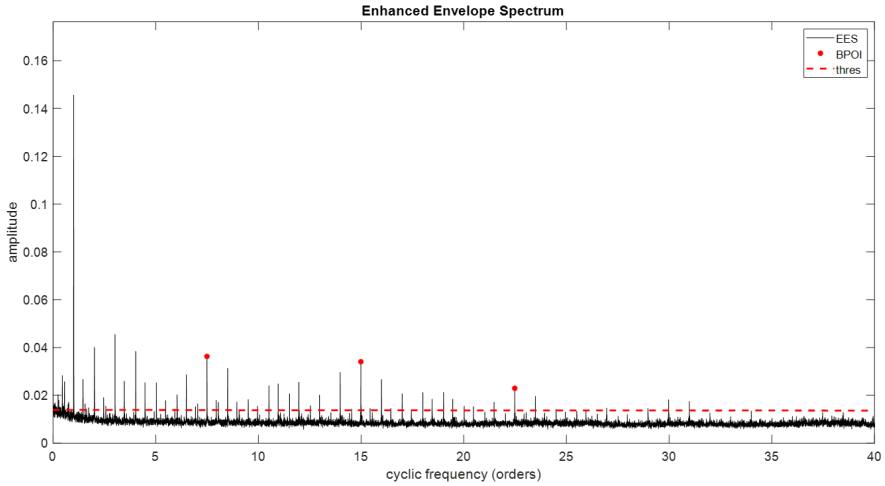

Figure 9: Enhanced Envelope Spectrum from the OFCMS of the smartphone acoustic signal for the large outer race damage case.

Lastly, a bearing in healthy conditions is also tested as a benchmark. The acoustic signals and the estimated speed and reference speed are shown in Fig. 10. Here it can be seen that the proposed method estimated the speed accurately for this case, as the deviation between reference and estimated speeds is minimal. The resulting OFCMS and EES exhibit the shaft speed as a very deterministic and high peak, above the noise level, as can be seen in Fig. 11.

5 Conclusion

This paper proposed the use of smartphone audio and video data for shaft speed estimation and bearing diagnostics.

Smartphone video acquisition of a rotating shaft with a zebra pattern glued to the shaft using a smartphone is proposed for rotating speed estimation. The method takes advantage of the rolling shutter effect to acquire the

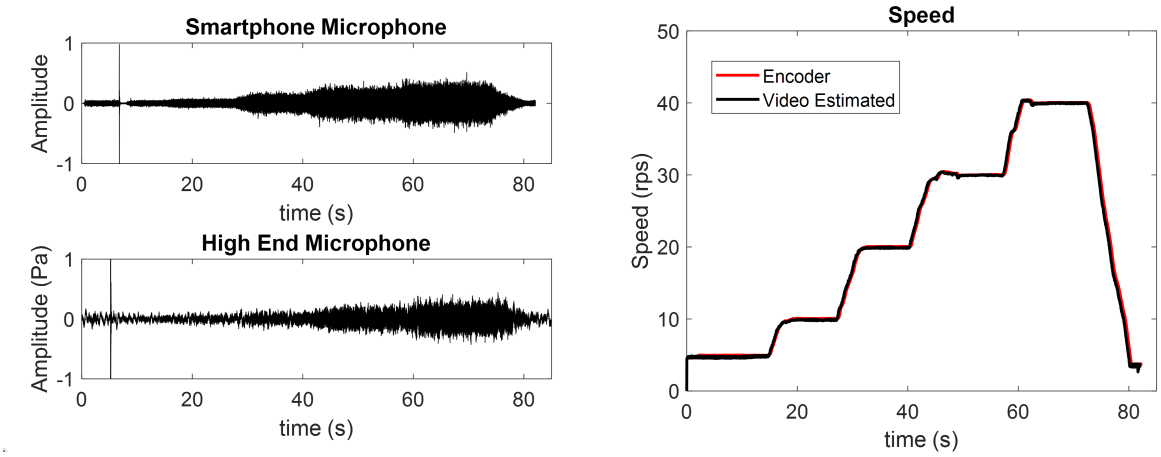

Figure 10: (left) Acoustic signals from high end and smartphone microphones and (right) speed from image processing estimation and reference speed from encoder.

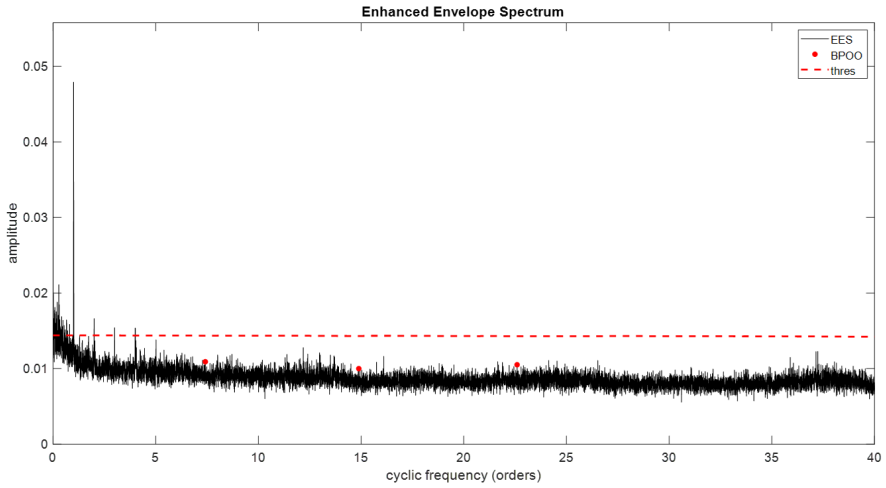

Figure 11: (left) Acoustic signals from high end and smartphone microphones and (right) speed from image processing estimation and reference speed from encoder.

speed above the Nyquist of the video frame rate. Calibration of the distance to the shaft, its diameter, rolling shutter period are needed in order to estimate accurately the rotating speed. This image processing method is described and validated using real video data acquired on a rotating shaft under varying speed conditions between 5 rps and 40 rps.

Smartphone audio signals are proposed for bearing diagnostics under varying speed conditions. Using the speed estimated via image processing method, the Order-Frequency Cyclic Modulation Spectrum exhibiting the bearing fault related orders can be extracted. Integration of the map to obtain the Enhanced Envelope Spectrum is also proposed for bearing diagnostics. The method was validated using real data acquired from 3 cases: Large Outer Race damage; Mild Inner Race damage: and Healthy conditions. The proposed method was seen to provide robust bearing diagnostics for all cases.

Acknowledgements

This research was supported by Flanders Make, the strategic research centre for the manufacturing industry and VLAIO in the frames of the ACMON ICON project. The authors would like to acknowledge the support of the Fonds Wetenschappelijk Onderzoek Vlaanderen (FWO) under the research grant no. 1SE0123N.

References

[1] W. Smith, Z. Fan, Z. Peng, H. Li, R. Randall, *Optimised spectral kurtosis for bearing diagnostics under electromagnetic interference*, Mech. Syst. Sig. Process., 75:371-394, 2016.

[2] J. Antoni, G. Xin, N. Hamzaoui, *Fast computation of the spectral correlation*, Mech. Syst. Sig. Process., 92:248-277, 2017.

[3] D. Abboud, S. Baudin, J. Antoni, D. Remond, M. Eltabach, O. Sauvage, *The spectral analysis of cyclo-non-stationary signals*, Mech. Syst. Sig. Process., 75:280-300, 2016.

[4] D. Abboud, J. Antoni, *Order-frequency analysis of machine signals*, Mech. Syst. Sig. Process., 87:229-258, 2017.

[5] A. Glowacz, *Fault diagnosis of single-phase induction motor based on acoustic signals*, Mech. Syst. Sig. Process., 117(15):65-80, 2019.

[6] A. Mauricio, H. Denayer, K. Gryllias., *Time-domain beamformed envelope spectrum of acoustic signals for bearing diagnostics*, Proceedings of ISMA2022-USD2022, Leuven, Belgium, 2022 September 12-14.

[7] E. Cardenas Cabada, Q. Leclere, J. Antoni, N. Hamzaoui, *Fault detection in rotating machines with beamforming: Spatial visualization of diagnosis features*, Mech. Syst. Sig. Process., 97:33-43, 2017.

[8] A. Mauricio, H. Denayer, K. Gryllias., *Beamformed envelope spectrum of acoustic signals for bearing diagnostics under varying speed conditions*, Proceedings of NOVEM, Auckland, New Zealand, 2023 January 10-12.

[9] C. Zhang, R. Wang, L. Yu, Y. Xiao, *Order domain beamforming for the acoustic localization of rotating machinery under variable speed working conditions*, Mech. Syst. Sig. Process., 205:109290, 2023.

[10] H. Andre , Q. Leclere, D. Anastasio, Y. Benaicha, K. Billon, M. Birem, F. Bonnardot, Z.Y. Chin, F. Combet, P.J. Daems, A.P. Daga, R. De Geest, B. Elyousfi, J. Griffaton, K. Gryllias, Y. Hawwari, J. Helsen, F. Lacaze, L. Laroche, X. Li, C. Liu, A. Mauricio, A. Melot, A. Ompusunggu, G. Paillot, S. Passos, C. Peeters, M. Perez, J. Qi, E.F. Sierra-Alonso, W.A. Smith, X. Thomas, *Using a smartphone camera to analyse rotating and vibrating systems: Feedback on the SURVISHNO 2019 contest*, Mech. Syst. Sig. Process., 154, June 2021.

[11] T. Verwimp, K. Gryllias., *Rotating Machinery Speed Extraction through Smartphone Video Acquisition*, KU Leuven, Leuven, Belgium, 2021 May.

[12] T. Verwimp, A. Mauricio, K. Gryllias., *Measurement of the speed of a rotating shaft through smartphone video acquisition exploiting the rolling shutter effect*, Proceedings of ISMA2022-USD2022, Leuven, Belgium, 2022 September 12-14.

[13] A. Mauricio, H. Denayer, K. Gryllias., *Cyclostationary tools to enhance relevant acoustic signals for bearing diagnostics*, Proceedings of NOVEM, Auckland, New Zealand, 2023 January 10-12.